Biomedical Research 2022; 33 (9): 264-269

ISSN 0970-938X
www.biomedres.info

Effect of radiation on Hydroxyapatite-Chitosan-Gelatin-Agarose scaffold for bone tissue regeneration.

Md. Masud Rana, Md. Arifuzzaman, Md. Shamim Miah, Naznin Akhtar, Sikder M Asaduzzaman*

Institute of Tissue Banking and Biomaterial Research, Atomic Energy Research Establishment, Dhaka-1349, Bangladesh

Abstract

Development of tissue engineering scaffolds with native-like microarchitectures is an essential for generation of tissues. To overcome the bounds of traditional bone substitutes, hydroxyapatite and biodegradable polymer composites are taken attention for bone tissue regeneration. The main aim of this study was to fabricate a biomimetic scaffold through thermally induced phase separation technique, cross-linked with irradiation and evaluated their efficiency for bone tissue restoration. The fabricated scaffold was characterized by porosity, swelling kinetics, biodegradability, physicochemical interaction within the components and morphological properties. The porosity of the scaffold was measured by liquid displacement method, chemical structure was analyzed by fourier transform infrared analysis, morphological analysis was performed by light microscopic analysis etc. Among the fabricated scaffolds, cross linked with 25 kGy radiation doses scaffold was found to be more eligible for bone replacement due to its acceptable porosity, biodegradability and swelling ability. FTIR analysis also showed intermolecular interaction between components of the scaffold. Considering the light microscopic analysis of HCGA, it was found that the scaffold was porous and pores were interconnected for cell migration and regeneration.

Keywords: Tissue engineering, Scaffold, Radiation, Cross-linker, Hydroxyapatite.

Accepted on November 18, 2022

Introduction

Tissue engineering is defined as the process of combining scaffolds, cells, and the appropriate biochemical elements to create functional tissues that enhance or sustain organ function [1-4]. Its aim is to lessen the negative effects of conventional clinical therapies related to autografting (donor site morbidity and insufficiency of donor etc.,) and allografting (immunogenic reaction, risk of diseases transmission, less consistence etc.,) [5,6]. When developing an artificial bone matrix, a tissue engineering scaffold is crucial for healing bone tissue and producing the best environment for tissue growth and regeneration [7,8]. In order to achieve adequate nutrient transport and cell proliferation, scaffolds must therefore have a few unique characteristics, such as nontoxicity, biodegradability, a suitable surface chemistry, an interconnected porous network, a suitable pore size, and a suitable shape [9,10]. In the application of bone tissue engineering, choosing the suitable material to create a scaffold is a crucial step [11]. Materials that are frequently utilized in tissue engineering include hydroxyapatite, b-TCP, collagen, gelatin, alginate, polycaprolactone, carboxy methyl cellulose, carbon nanotubes, agarose, montmorillonite, and so on as polymer sources [12-16].

Hydroxyapatite (HA) is a vital biomaterial for making scaffolds. It can be made from a variety of naturally occurring sources with calcium-based structures, including bone, mollusk shells, coral, etc., [17,18] and is similar in chemical composition to the mineral found in human bone tissue. It is also thought to be crucial for a number of biomedical applications [7,19-22].

Chitosan is another popular natural biopolymer utilized for bone tissue engineering. It is an N-acetyl glucosamine and glucosamine-based linear polysaccharide. Chitin is deacetylated to produce it. Chitosan is a sought-after substance for biomedical applications due to its tissue compatibility, antibacterial activity, bioresorbability, and hemostatic properties [23-25]. Furthermore, the degraded forms of chitosan are not poisonous, immune-stimulating, or carcinogenic [26].

Collagen, a fibrous protein that is widely distributed throughout the animal kingdom in the form of hides, skins, bones, and connective tissues, is the source of gelatin, a water-soluble, protein-based natural biopolymer [27]. It has been utilized for many years in pharmaceutical formulation because of its biocompatibility, biodegradability, and affordability. It has been employed for many years in

pharmaceutical formulation, cell culture, and tissue engineering applications due to its biocompatibility, biodegradability, and low cost of availability [28-30].

Agarose is a biocompatible linear polysaccharide that is produced from marine red algae. It has similar mechanical qualities to those needed for tissues and can be easily regulated by modifying its composition. Agarose has been regarded as a viable contender for usage in biomaterials due to its biodegradability, renewability, and strong gelling power [31,32]. Utilizing each individual component in material mixing is a successful strategy for obtaining materials with optimum functional qualities, and significant advancements have been made in the use of bone tissue engineering [33-35].

Crosslinking of scaffold is currently one of the most important fields in biomedical research. By creating a stable network in the polymeric matrix, crosslinking's main purpose is to enhance the biomechanical capabilities of scaffolds [36]. A crosslink is a covalent bond or supra-molecular contact, such as an ionic bond or hydrogen bond, that joins the functional groups of a polymer chain to another one [37]. A crosslinker must not only have no cytotoxic effects but also enhance the mechanical properties of the polymer network in order to be considered ideal [38]. Crosslinking of scaffolds by irradiation-based methods is accomplished using high-energy ionizing radiation or photo initiator molecules. This method is frequently employed to crosslink collagen scaffolds [39,40]. During irradiation by Ultraviolet (UV) radiation, there are two opposite and competitive processes namely, UV-induced crosslinking and UV-induced denaturation, and the balance between them is essential for the fabrication of scaffolds. The mechanical performance and degrading behavior of irradiation scaffolds are ultimately affected by this balance [41,42]. This study's primary objective was to create a biomimetic scaffold using the Thermally Induced Phase Separation (TIPS) technique, cross-linked with various radiation dosages, and then assess its attributes for the effectiveness of bone tissue engineering.

Materials and Methods

Fabrication of scaffold

In this study, scaffolds were prepared by following our previous work [10]. In short, bovine derived HA was weighed into a flask and added deionized water. After being stirred for two hours at room temperature, mixture was ultrasonically treated to fully disperse the HA powder into the water.

Chitosan solution was prepared by mixing chitosan in 1% acetic acid solution. Then gelatin was added to the chitosan solution at 1:2 ratio and the solution was agitated at 37°C to form a chitosan gelatin blend. After stirring this mixture was placed into water bath at 40°C temperature. Afterward, HA was added to the chitosan-gelatin mixture and stirred for 2 hours to disperse thoroughly. Finally, agarose solution was added separately into the prepared solution and stirred for 2 hours to disperse properly. The resulting solution was put into specific mold and pre-frozen for 24 hours at -40°C followed by freeze-drying at (-50°C ~ -60°C) for 30 hours to obtain porous scaffolds.

Characterization of scaffold

Porosity: The liquid displacement method was used to determine the porosity of the constructed scaffolds. In this investigation, ethanol was used as solution. A sample of known Weight (W) was immersed in a graduated cylinder filled with a known volume of ethanol (V1) for 5 minutes. The ethanol-soaked scaffold had a total in-cylinder volume of V2. The ethanol-impregnated scaffold was removed from the cylinder and the amount of ethanol remaining was measured (V3). In triplicate, each sample was measured. The scaffolds' porosity (Є) is expressed as follows.

$$Є = (V1 - V3)/(V2 - V3)$$

Swelling ratio evaluation: Swelling capacity was calculated using water absorption. The dry weight of the scaffold was taken as W_0. The porous scaffolds were then soaked in pH 7.4 PBS buffer for 24 hours at 37°C. The scaffolds were then removed from the PBS buffer and their wet weight (Ww) recorded. Equation was used to compute the swelling ratio.

$$Swelling\ ability\ (\%) = \frac{W_w - W_0}{W_0} \times 100$$

***In-vitro* biodegradability:** The biodegradability of the scaffolds was evaluated by soaking the scaffolds in PBS medium containing lysozyme (10,000 U/ml) at 37°C for 21 days at several intervals. The initial scaffold weight was represented as W_0. After the particular days, the scaffolds were picked up from the solution and washed with deionized water to remove ions adsorbed on the surface and then freeze-dried. The dry weight of the scaffold was symbolized as Wt. The biodegradation of the fabricated scaffolds was evaluated using following equation.

$$Biodegradability\ (\%) = \frac{W_0 - W_t}{W_t} \times 100$$

Fourier Transform Infrared Spectroscopy (FTIR) analysis: FTIR Spectroscopy, is a systematic technique used to identify organic, polymeric, and in some cases, inorganic materials. This method uses infrared light to scan test samples and observe chemical properties. In this study, the scaffold samples were evaluated by FT-IR 8400S spectrophotometer (Shimadzu, Japan) within 4000-700cm^{-1} range at 4 cm^{-1} resolution.

Pore morphology: The morphology of the scaffolds were observed using light optical microscopy (Leica, Germany).

Results and Discussion

General observation

In this study, HA-Chitosan-Gelatin-Agarose (HCGA) scaffolds were fabricated by thermally induced phase

separation technique and cross-linked by physical cross linkers (gamma radiation). This choice of manufacturing technique resulted in a scaffold with excellent porosity. This is brought about by the formation of ice crystals during freezing and their subsequent removal during freeze-drying. The fabricated HCGA scaffold turned out to be a rigid structure with a spongy appearance.

FTIR analysis

FTIR analysis states us the chemical interactions among the constituents of scaffold. When diverse materials are mixed together, the variations in characteristic peaks of the infrared spectrum can reveal whether there are chemical interactions among them. In HCGA scaffold, agarose was validated owing to the presence of peaks at 930 cm^{-1} owing to 3,6-anhydrogalactose. Peak at 1075 cm^{-1} is enriched in the blend, which is owing to the glycosidic linkages in the polymers [16]. A small number of other peaks are also overlapping that can be due to the analogous functional groups in the polymers (Figure 1). In the FTIR result, HA showed the presence of -OH group at around 3200-3429 cm^{-1} due to the water absorption ability, the presence of CO_3^{2-} group was at around 1410-1450 cm^{-1} and 873 cm^{-1} that matched with human bone analysis [43]. For phosphate group, it was appeared at 1029-1095 cm^{-1} and 962 cm^{-1}-560 cm^{-1}. The phosphate group can be v4 PO_4^{3-} bend and v1 PO_4^{3-} and v2 CO_3^{2-} bend principally. The presence of standard v3 CO_3^{2-} is at the wave number between 1460-1580 cm^{-1} and 800-871 cm^{-1}; so the existence of v3 CO_3^{2-} was found at 1452 cm^{-1} was desired. The spectrum of bone exhibits all the most intense bands observed in the spectrum of hydroxyapatite as the spectra herein showed. The broad absorption band of chitosan between 3600 and 3000 cm^{-1} could be attributed to the -OH and -NH stretching vibrations, the absorption bands at 1660, 1592, and 1385 cm^{-1} are respectively ascribed to the amide I, II and III bands, and the absorption band at 1068 cm^{-1} was attributed to the C-O stretching vibrations. Gelatin bands were found differently due to its different amide group and lysine, proline side chains. The primary amide band A is found at around 3500 cm^{-1}, N-H stretching band was distributed at 3535 cm^{-1}, C-H stretching at ~3327 cm^{-1} for the amide B, C=O stretching at 1637 cm^{-1} for the primary amide I, N-H deformation at 1500-1550 cm^{-1} for the amide II due to the physical cross-linking in the compound itself. Gelatin groups deformed at 1500-1550 cm^{-1} due to their intra cross-linking [44]. There was an absent band in gelatin amide II at 1546 cm^{-1} because it involved in the cross-linking reaction. The carboxyl group from gelatin and the Ca^{+2} ions from HA were the evidence of bond formation. Complex reaction between Ca^{2+} ions of HA and gelatin molecules was responsible for the binding. The Ca^{2+} ions of complex gelatin molecules assembled with PO_4^{3-} ions from HA. The -COOH and -NH_2 groups in the gelatin molecule form chemical bonds with P-O and O-H groups of HA, resulting in gelatin chains firmly attaching to the surface of HA [45].

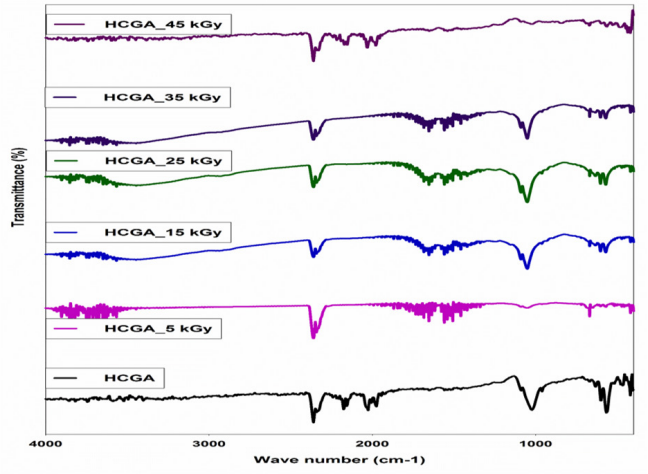

Figure 1. *FTIR spectra of the irradiated cross-linked scaffolds.*

In the spectrum for agarose film, the absorption band at 1641 cm^{-1} was ascribed to O-H bending, at 1075 cm^{-1}, attributed to the C-O stretching vibrations. The characteristic absorption bands of 3,6-anhydrogalactose and the C-H bending vibrations of anomeric carbon appeared at 931 and 890 cm^{-1}, respectively [16].

Porosity of the scaffolds

This high degree of porosity would allow cells to migrate into and populate within the scaffold. Porosity of the prepared scaffolds was measured through the liquid displacement method using ethanol. The porosity of the HCGA scaffold was 89.6%. When it was cross-linked through radiation, the porosity was ranged from 80%-88% at different radiation doses (Figure 2A) while cancellous bone porosity ranges from 30% to 90 % (mostly in the range 75%-95%) [46]. This might be due to little crosslinking ability of lower doses which caused the porosity to decrease a little.

Greater than 80% porosity changed into found for the polymeric scaffold, which could be an additional benefit for tissue engineering purposes [47]. High porosity with homogeneous, small cells replicates excessive nucleation charge whilst suppressing the impact of anisotropic boom of ice crystals [48]. This moderate porosity could permit cells to emigrate into and populate within the scaffold.

Swelling evaluation

The swelling capacity of a scaffold is a vital characteristic that causes an explosion in pore sizes that compare its realistic use in facilitating the attachment and progression of cells and the following new tissue regeneration [49]. The excessive water uptake potential of the composite scaffold might be attributed to the hydroxyl, amino and carboxyl hydrophilic companies that exist within the polymer [50]. The outcomes confirmed that there are variations in the swelling conduct some of the scaffolds, in which the water uptake capacity of the non-cross-connected HCGA scaffold changed into better while as compared to

cross-connected scaffold (Figure 2B). It's can be due to the fact at decrease radiation dose the crosslinking wasn't robust sufficient so the polymers had the hazard to swell, but growing radiation dose will increase its crosslinking potential and so at better doses improved crosslinking decreased the intermolecular area and reduced swelling charge [51].

Evaluation of biodegradability

Degradation performances of porous scaffolds play a crucial role in the engineering progression of a new tissue. The biodegradation of scaffolds provides space for tissue growth and matrix deposition. An ideal rate would be that which corresponds to the regeneration of new bony structure in order to provide a smooth transition [16]. In the case of biodegradation, uncross-linked scaffold had the highest degradation rate which reduced gradually with increasing radiation dose. Scaffold irradiated at 5 kGy had degradation rate very similar to that of the uncross-linked scaffold this is because at lower radiation dose degradation of scaffold occur more frequently with a little crosslinking (Figure 2C). However increasing radiation dose decreases the degradation and increases the crosslinking capacity [51].

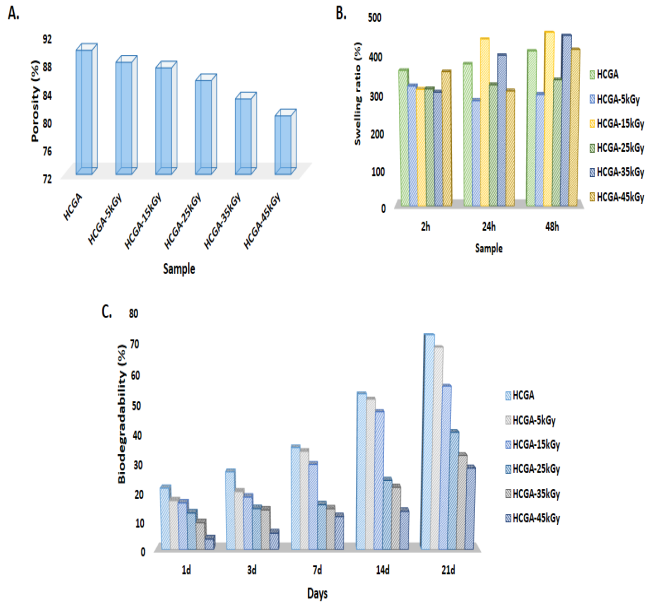

Figure 2. *Physical properties of the irradiated cross-linked scaffolds. (A) Porosity; (B) Swelling ratio; and (C) Biodegradability.*

Pore morphology analysis

The pore morphology is between oval and polygonal. The size and density of the holes is not consistent. The formation of the holes is partly due to the rupture of the pore walls between the gaps left by the ice sublimation in the frozen composite during the freeze drying process. The micro-pore structures of the scaffold were of great benefit to cell regeneration and reproduction, evidencing this matrix great development prospects in the field of biomedical materials (Figure 3).

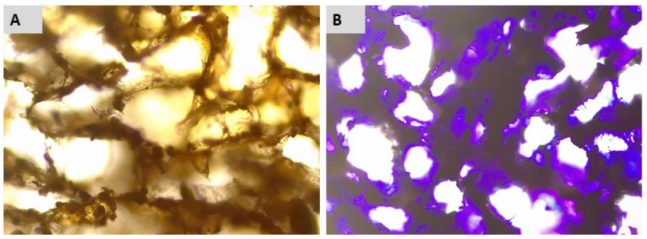

Figure 3. *Microscopic analysis of the scaffolds. (A) HCGA scaffold; (B) HCGA scaffold staining by crystal violet.*

The optimal pore size for bone tissue engineering remains unknown. However, a study aimed at determining the optimal pore size for bone tissue engineering showed that pore sizes in the range of 80-500 µm were feasible [52]. Due to the depicted pore size, the scaffolds allow cell attachment, proliferation, and nutrient delivery, allowing for proper bone tissue growth. Optical microscopy images revealed that the distribution of components within the scaffold network was uniform in the fabricated scaffolds.

Conclusion

The purpose of this study was to determine the ideal radiation dose for fabricating porous scaffolds using HA, chitosan, gelatin, and agarose materials that have desirable porosity, swelling ratio, biodegradability, and pore morphology for cell growth and proliferation. At 25 kGy doses of scaffold, light microscopy revealed an open pore structure that was suitable for blood supply and cell adhesion. These irradiated porous scaffolds are promising candidates for bone tissue formation.

Acknowledgement

The authors would like to thank the International Atomic Energy Agency (IAEA) for their support to carry out this work as a part of Coordinated Research Project (CRP project no. 18343/R1).

Conflict of Interest

The authors declare that there is no conflict of interest regarding the publication of this paper.

References

1. Reichert JC, Cipitria A, Epari DR, Saifzadeh S, Krishnakanth P. A tissue engineering solution for segmental defect regeneration in long bones. Sci Transl Med 2012; 4: 141ra93.
2. Castells-Sala C, Alemany-Ribes M, Fernandez-Muiños T, Recha-Sancho L, Lopez-Chicon P. Current applications of tissue engineering in biomedicine. J Biochip Tissue chip 2013; S2: 004.
3. Bajaj P, Schweller RM, Khademhosseini A, West JL, Bashir R. 3D biofabrication strategies for tissue engineering and regenerative medicine. Annu Rev Biomed Eng 2014; 16: 247-276.
4. Moroni L, Burdick JA, Highley C, Lee SJ, Morimoto Y, Takeuchi S, Yoo JJ. Biofabrication strategies for 3D *in vitro* models and regenerative medicine. Nat Rev Mater 2018; 3: 21-37.

5. Fishman JA, Greenwald MA, Grossi PA. Transmission of infection with human allografts: Essential considerations in donor screening. Clin Infect Dis 2012; 55: 720-727.
6. Jan H, Woodruff MA, Epari DR, Steck R, Glatt V, Dickinson IC, Choong PFM, Schuetz MA, Hutmacher DW. Bone regeneration based on tissue engineering conceptions: A 21st century perspective. Bone Res 2013; 1: 216-248.
7. Dhandayuthapani B, Yoshida Y, Maekawa T, Kumar DS. Polymeric scaffolds in tissue engineering application: A review. Int J Poly Sci 2011; 2011: 1-19.
8. Katari R, Peloso A, Orlando G. Tissue engineering and regenerative medicine: Semantic considerations for an evolving paradigm. Front Bioeng Biotechnol 2015; 2: 57.
9. Hollister SJ. Porous scaffold design for tissue engineering. Nat Mater 2005; 4: 518-524.
10. Sultana T, Rana MM, Akhtar N, Hasan MZ, Talukder AH, Asaduzzaman SM. Preparation and physicochemical characterization of nano-hydroxyapatite based 3d porous scaffold for biomedical application. Adv Tissue Eng Regen Med: Open Access 2017; 3: 00065.
11. Salgado AJ, Oliveira JM, Martins A, Teixeira FG, Silva NA, Neves NM, Sousa N, Reis RL. Tissue engineering and regenerative medicine: Past, present, and future. Int Rev Neurobiol 2013; 108: 1-33.
12. Venkatesan J, Qian ZJ, Ryu B, Kumar AN, Kim SK. Preparation and characterization of carbon nanotube-grafted-chitosan: Natural hydroxyapatite composite for bone tissue engineering. Carbohydrate Polymer 2011; 83: 569-577.
13. Li J, Chen Y, Yin Y, Yao F, Yao K. Modulation of nano-hydroxyapatite size *via* formation on chitosan–gelatin network film in situ. Biomaterials 2007; 28: 781-790.
14. Zhang L, Tang P, Zhang W, Xu M, Wang Y. Effect of chitosan as a dispersant on collagen-hydroxyapatite composite matrices. Tissue Eng Part C Methods 2010; 16: 71-79.
15. Xiao X, Liu R, Huang Q, Ding X. Preparation and characterization of hydroxyapatite/ polycaprolactone-chitosan composites. J Mater Sci Mater Med 2009; 20: 2375-2383.
16. Rana MM, Akhtar N, Rahman MS, Jamil HM, Asaduzzaman SM. Extraction of hydroxyapatite from bovine and human cortical bone by thermal decomposition and effect of gamma radiation: A comparative study. Int J Comple Alt Med 2017; 8: 00263.
17. Vecchio KS, Zhang X, Massie JB, Wang M, Kim CW. Conversion of bulk seashell to biocompatible hydroxyapatite for bone implants. Acta Biomater 2007; 3: 910-918.
18. Barakat NAM, Khalil KA, Sheikh FA, Omran AM, Gaihre B, Khil SM, Kim HY. Physiochemical characterization of hydroxyapatite extracted from bovine bones by three different methods: Extraction of biologically desirable hap. Mat Sci Eng 2008; 28: 1381-1387.
19. Ramos AP, Cruz MAE, Tovani CB, Ciancaglini P. Biomedical applications of nanotechnology. Biophys Rev 2017; 9: 79-89.
20. Kruger TE, Miller AH, Wang J. Collagen scaffolds in bone sialoprotein-mediated bone regeneration. Scientific World Journal 2013; 812718.
21. Thrivikraman G, Madras G, Basu B. *In vitro*/ *In vivo* assessment and mechanisms of toxicity of bioceramic materials and its wear particulates. RSC Adv 2014; 4: 12763-12781.
22. Fahmy MD, Jazayeri HE, Razavi M, Masri R, Tayebi L. Three-dimensional bioprinting materials with potential application in preprosthetic surgery. J Prosthodont 2016; 25: 310-318.
23. Cheung RCF, Ng TB, Wong JH, Chan WY. Chitosan: An update on potential biomedical and pharmaceutical applications. Mar Drugs 2015; 13: 5156-5186.
24. Hurt AP, Kotha AK, Trivedi V, Coleman NJ. Bioactivity, biocompatibility and antimicrobial properties of a chitosan-mineral composite for periodontal tissue regeneration. Polímeros 2015; 25: 3.
25. Henríquez CMG, Vallejo, MAS, Hernandez JR. Advances in the fabrication of antimicrobial hydrogels for biomedical applications. Materials 2017; 10: 232.
26. Marin E, Briceño MI, George CC. Critical evaluation of biodegradable polymers used in nanodrugs. International J Nano Med 2013; 8: 3071-3091.
27. Panzavolta S, Fini M, Nicoletti A, Bracci B, Rubini K. Porous composite scaffolds based on gelatin and partially hydrolyzed α-tricalcium phosphate. Acta Biomater 2006; 5: 636-643.
28. Senthilarasan K, Ragu A, Sakthivel P. Synthesis and characterization of hydroxyapatite and gelatin doped with magnesium chloride for bone tissue engineering. Int J Eng Res Tech 2014; 3: 1-5.
29. Lai JY. Biocompatibility of chemically cross-linked gelatin hydrogels for ophthalmic use. J Mater Sci Mater Med 2010; 21: 1899-1911.
30. Rose JB, Pacelli S, El Haj AJ, Dua HS, Hopkinson A, White LJ, Rose FRAJ. Gelatin-based materials in ocular tissue engineering. Materials (Basel) 2014; 7: 3106-3135.
31. Deszczynski M, Kasapis S, Mitchelle JR. Rheological investigation of the structural properties and aging effects in the agarose/co-solute mixture. Carbohydrate Polymers 2003; 53: 85-93.
32. Lahooti S, Sefton MV. Effect of an immobilization matrix and capsule membrane permeability on the viability of encapsulated HEK cells. Biomaterials 2000; 21: 987-995.
33. Shih CM, Shieh YT, Twu YK. Preparation and characterization of cellulose/chitosan blend films. Carbohydrate Polymers 2009; 78: 169-174.
34. Ke G, Xu W, Yu W. Preparation and properties of drug-loaded chitosan–sodium alginate complex membrane. Int J Poly Mater 2010; 59: 184-191.
35. Liu F, Qin B, He L, Song R. Novel starch/chitosan blending membrane: Antibacterial, permeable and mechanical properties. Carbohydrate Polymers 2009; 78: 146-150.
36. Daemi H, Barikani M. Synthesis and characterization of calcium alginate nanoparticles, sodium homopolymannuronate salt and its calcium nanoparticles. Scientia Iranica 2012; 19: 2023-2028.
37. Daemi H, Barikani M, Sardon H. Transition-metal-free synthesis of supramolecular ionic alginate-based polyurethanes. Carbohydrate polymers 2017; 157: 1949-1954.
38. Suzuki A, Sasaki S. Swelling and mechanical properties of physically crosslinked poly (vinyl alcohol) hydrogels. Proc Inst Mech Eng H 2015; 229: 828-844.

39. Davidenko N, Schuster CF, Bax DV, Raynal N, Farndale RW, Best SM, Cameron RE. Control of crosslinking for tailoring collagen-based scaffolds stability and mechanics. Acta Biomater 2015; 25: 131-142.
40. Zhang X, Xu L, Wei S, Zhai M, Li J. Stimuli responsive deswelling of radiation synthesized collagen hydrogel in simulated physiological environment. J Biomed Mater Res A 2013; 101: 2191-2201.
41. Davidenko N, Bax DV, Schuster CF, Farndale RW, Hamaia SW, Best SM, Cameron RE. Optimisation of UV irradiation as a binding site conserving method for crosslinking collagen-based scaffolds. J Mater Sci Mater Med 2016; 27: 14.
42. Manas D, Ovsik M, Mizera A, Manas M, Hylova L, Bednarik M, Stanek M. The effect of irradiation on mechanical and thermal properties of selected types of polymers. Polymers (Basel) 2018; 10: 158.
43. Figueiredo MM, Gamelas JAF, Martins AG. Characterization of bone and bone-based graft materials using FTIR spectroscopy. Infrared Spectroscopy-Life and Biomedical Sciences 2012; 18: 378.
44. You F, Wu X, Chen X. 3D printing of porous alginate/gelatin hydrogel scaffolds and their mechanical property characterization. Int J Poly Mater Poly Biomater 2017; 66: 299-306.
45. Tontowi AE, Perkasa DP, Siswomihardjo W, Darwis D. Effect of Polyvinyl Alcohol (PVA) blending and gamma irradiation on compressive strength of FHAp/FGel composite as candidate of scaffold. Int J Eng Tech 2016; 8: 108-116.
46. Cowin SC, Cardoso L. Blood and interstitial flow in the hierarchical pore space architecture of bone tissue. J Biomech 2015; 48: 842-854.
47. Foroughi AH, Razavi MJ. Multi-objective shape optimization of bone scaffolds: Enhancement of mechanical properties and permeability. Acta Biomater 2022; 146: 317-340.
48. Xie X, Zhou Y, Bi H, Yin K, Wan S, Sun L. Large-range Control of the microstructures and properties of three-dimensional porous graphene. Sci Rep 2013; 3: 2117.
49. Wang L, Nan X, Hou J, Xia Y, Guo Y, Meng K, Xu C, Lian J, Zhang Y, Wang X, Zhao B. Preparation and biological properties of silk fibroin/nano-hydroxyapatite/hyaluronic acid composite scaffold. Biomed Mater 2021; 16.
50. Ahmadi F, Oveisi Z, Samani SM, Amoozgar Z. Chitosan based hydrogels: Characteristics and pharmaceutical applications. Res Pharm Sci 2015; 10: 1-16.
51. Islam MM, Zaman A, Islam MS, Khan MA, Rahman MM. Physico-chemical characteristics of gamma-irradiated gelatin. Prog Biomater 2014; 3: 21.
52. Chen Z, Yan X, Yin S, Liu L, Liu X, Zhao G, Ma W, Qi W, Ren Z, Liao H, Liu M, Cai D, Fang H. Influence of the pore size and porosity of selective laser melted Ti6Al4V ELI porous scaffold on cell proliferation, osteogenesis and bone ingrowth. Mater Sci Eng C Mater Biol Appl 2020; 106: 110289.

***Correspondence to:**

Sikder M Asaduzzaman

Institute of Tissue Banking and Biomaterial Research

Atomic Energy Research Establishment

Dhaka-1349

Bangladesh